International Journal of Energetica (IJECA)
https://www.ijeca.info
ISSN: 2543-3717 Volume 6. Issue 1. 2021 *Page 18-24*

Influence of the geographical parameters on the performance of hybrid solar gas turbine

Omar Behar[1,2], Basim Belgasim[3,4] Daniel Sbarbaro[1,2], Luis Moran[1,2]

[1]*Solar Energy Research Center (SERC-Chile), Santiago de Chile, CHILE*
[2]*Department of electrical engineering, University of Concepcion, Concepcion, CHILE*
[3]*Center for Solar Energy Research and Studies, Tripoli, LIBYIA*
[4]*Mechanical Engineering Department, University of Benghazi, Benghazi, LIBYIA*

Email* : *beharomar@gmail.com*

Abstract – *This study aims to investigate the influence of the geographical and climate parameters on the performance of the hybrid solar gas turbine with a pressurized air receiver. A number of sites located in South America (Chile, Bolivia, and Peru) and North Africa (Algeria and Libya) are considered. The geometric design parameters of the solar receiver and the tower are calculated using an in-house code. The layout and the optical performance of the heliostat field are carried out using SolarPILOT software. The simulation of the complete hybrid solar gas turbine is carried out using TRNSYS software. A 50 MWe hybrid solar gas turbine is chosen in this study. Results show that a hybrid solar gas turbine installed in North Africa performs better than that installed in South America. This is mainly due to the optical performance of the heliostat field, which are better in North Africa are than in South America. The highest annual optical efficiency of a solar field is observed at Bechar (Algeria) 56.8% while the lowest annual efficiency is observed at Antofagasta (Chile) 48.1%.The solar-to-electric efficiency at Atacama Desert is lower than in the Sahara Desert. Indeed, in Atacama region the solar-to-electric efficiency varies from 17% at Antofagasta to about 18% in Arequipa while it is above 19% at Sabha and Bechar.*

Keywords: *Solar energy, hybrid solar gas turbine, solar thermal power plants, concentrating solar power, solarPILOT, TRNSYS.*

Received: 30/04/2021 – Accepted: 15/06/2021

I. Introduction

Concentrating solar power has attracted a lot of interest due to its potential for integration with the conventional power conversion cycles including Rankine cycles and Brayton cycles [1]. The integration of the central receiver system with the Brayton cycles and combined cycles offers several advantages including high solar to electric conversion efficiency and scalability [2]. The concept that integrates the central receiver system with the Brayton cycle is known as Hybrid Solar Gas Turbine (HSGT). In a typical HSGT, concentrated solar heat is used to preheat the compressed air prior to combustion. Three research projects namely SOLGATE [3–5], SOLHYCO [6], and SOLUGAS [7, 8] have demonstrated the HSGT technology.

In small scale systems, the HSGT technology has been studied intensively by many researchers. Researchers have investigated the performance of micro HSGT systems under different operation conditions [9].

the performance of the GT based on a parabolic concentrator has been analysed for solar only and hybrid operation [10]. Technical, economic and environmental evaluation including thermal design were presented by an in-depth study [11]. Thermo-economic modelling and simulation were also provided [12]. The effect of inlet temperature on the performance of small scale HSGT systems were presented [13]. A thermodynamic and CFD modelling were presented for a small scale HSGT power generation unit [14]. A small scale solar tower integrated with gas turbine system has been presented [15]. Behar investigated an innovative design for the the preheating system of the HSGT plants [16]. Also, a thermal analysis of HSGT system integrated with parabolic dish collector was presented by a group of researchers [17]. A study investigated the domestic applications of the small scale HSGT systems based on axial turbine system [18]. Investigation predicted the simulation procedure of the performance of the HSGT systems [19]. Regarding to large scale HSGT systems, there is a clear shortage in the studies and research based on the previous literature. Recently study suggested a design methodology for the solar field of the large scale HSGT systems [20]. The study included modelling and simulation validated by real data from a case study.

This paper aims to investigate the influence of the geographical and climate parameters on the performance of commercial HSGTs integrated with heliostat solar filed and central pressurized air receiver. A number of sites located in South America and North Africa are selected. A simplified methodology is adopted to design the solar filed of each site and the optical performance is predicted using SolaPILOT simulation tool. The whole system is modelled using the well-known energy simulation tool TRNSYS 18 using the input data from the design process and optical analysis for each of the proposed locations of the study.

II. Methods and tools

II.1. A practical technique to design the solar receiver and the tower

The central receiver system includes the heliostat field, the solar receiver, and the tower. A practical technique is used to design the solar receiver and the tower. A cavity-type receiver is considered in this study. The nominal power of the receiver can be calculated using the following expression:

$$P_{nom\_rec} = \frac{SM.P_{nom\_pb}}{y_{nom\_pb}} \quad (1)$$

Where SM is the solar multiple, P refers to power, and η refers to the efficiency. Subscripts "nom" and "pb" refer to nominal and power block respectively.

The incident receiver power on the receiver from the heliostat field is a function of the receiver nominal efficiency:

$$P_{nom\_rec\_inc} = \frac{P_{nom\_rec}}{y_{nom\_rec}} \quad (2)$$

Subscripts "rec" and "inc" refer to the receiver and incident power respectively. The average allowable flux is calculated as:

$$F_{avg} = \frac{F_{peak}}{FR} \quad (3)$$

Where F_{avg} is the average heat flux, F_{peak} is the peak heat flux, and FR is the peak-to-average heat flux ratio.

The receiver area is calculated as:

$$A_{rec} = \frac{P_{nom\_inc}}{F_{avg}} \quad (4)$$

The radius of the receiver is given as:

$$R_{rec} = \sqrt{\frac{A_{rec}}{\frac{\theta_{rec}}{\pi}.\pi^2.HWR_{rec}}} \quad (5)$$

Where: θrec is the opening angle of the cavity. HWRrec is the height to width ratio of the receiver.

The height of the receiver is:

$$H_{rec} = 2.R_{rec}.HWR_{rec} \quad (6)$$

The width of the aperture of the receiver is

$$W_{ap} = 2.R_{rec}.\cos\left(\frac{\pi-\theta rec}{2}\right).AWR \quad (7)$$

Where: AWR is the aperture width to total width ratio.

The aperture height is

$$H_{ap} = 2.H_{rec}.AHR \quad (8)$$

Where: AHR is the aperture height to total height ratio. The tower height is estimated using the following expression:

$$H_{tower} = 0.6806.P_{nom\_rec} + 106.60 \quad (9)$$

P_{nom_rec} is in MW is the above equation.

II.2. The tool used to design the heliostat field

SolarPILOT is used to design the heliostat field. SolarPILOT software is dedicated to design and estimate the performance of the central receiver systems. It was developed as an extension to DELSOL3 with several improvements in the heliostat field layout, characterization, parametric simulation, plotting, and optimization of the central receiver system. It uses the analytical flux image Hermite series approximation and applies the analytical model to individual heliostat images. In addition, it uses a Monte-Carlo ray-tracing technique for the optical modeling of the solar receiver.

II.3. The tool used to design the simulate the complete system

TRNSYS is used to simulate the performance of the HSGT. TRNSYS is a simulation tool of time-dependent energy systems. It has a solar library, which includes some solar concentrating collectors such as the parabolic trough concentrator and central receiver system. The library named Solar Thermal Electricity Components (STEC) is useful to model and simulate the HSGT. It includes Rankin and Bryton cycles in addition to the central receiver system. The HSGT model is illustrated in Figure 1. It consists from three weather data file, heliostat solar field, central pressurized air receiver and Briton cycle components.

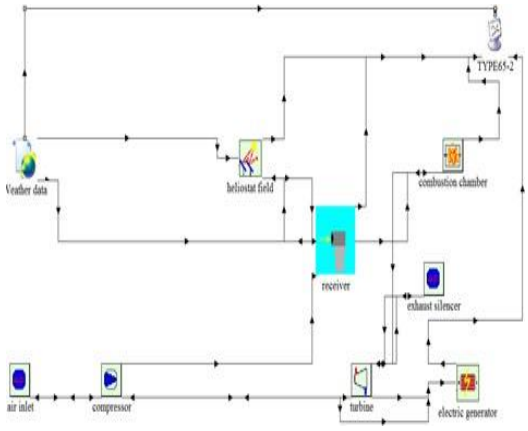

Figure 1. TRNSYS model of HSGT system.

III. Results and discussions

The locations proposed to be considered in this study are demonstrated in Table 1 including the country, latitude, longitude and time zone.

Table 1. Selected locations for the study

Country	**Time zone**
Chile	
Antofagasta (23°39'3.34"S 70°23'51.01"W) ele 16m	GMT -4
Peru	
Arequipa-Characa (16°30'26.19"S 71°31'15.30"W) ele 2782m	GMT -5
Bolivia	
Oruro-Juan-Mendoza (17°57'48.24"S 67° 4'23.77"W) ele 3709m	GMT -4
Algeria	
Bechar (31°37'25.72"N 2°12'58.48"W) ele 791m	GMT +1
Libya	
Sebha (27° 2'11.55"N 14°25'44.49"E) ele 426m	GMT +2

III.1. Results of heliostat field and receiver design

To calculate the geometric design parameters of the tower and the receiver, the nominal efficiency of the GT is taken as 37%. The nominal efficiency of the receiver is 80%. The receiver is supposed to be built with Incoloy 800H. The allowable peak flux is 1000 kW/m^2. A peak to average flux ratio of 1.78 is considered. The opening angle of the receiver is 180°. The aspect ratio of the receiver (height to diameter ratio) is 1.27.

The ratio of the height of the aperture to the height of the receiver is 0.9. The ratio of the width of the aperture to the total width of the receiver is 0.9. The solar multiple SM=1. Table 2 illustrates the design parameters of the central receiver system for a hybrid solar gas turbine of 50 MWe. The nominal power of the receiver is 135.14 MWth, its absorptive surface is 300.68 m^2. The aperture of the receiver is a rectangle of 11.20 m in height and 8.8 m in width. The height of the tower is 198.57 m. The reflective surface of the heliostat field is 248776.02 m^2.

Table 2. Design parameters of a heliostat field system for 50MWe solar gas turbine.

Parameter	**unit**	**Value**
Nominal power of the receiver	MW	135,14
Power intercept on the receiver	MW	168,92
Receiver absorbtive surface	m^2	300,68
Receiver height	M	12,44
Radius of the receiver	M	4,90
Width of the aperture	M	8,80
Height of the aperture	M	11,20
Aperture area	m2	98.71
Height of the tower	M	198,57
Reflective surface of the solar field	m2	248776,02

The layout and the optical performance of the heliostat field are carried out using SolarPILOT software. This software requires mainly the data of the location, the dimensions of a single heliostat, the geometric dimensions of the receiver and the tower, and the optical proprieties of the heliostat and the receiver. Figure 2 shows the layout and the annual optical efficiency of the heliostat field installed at the selected sites. The layout method is radial stagger and the sun location at the design point is the summer solstice.

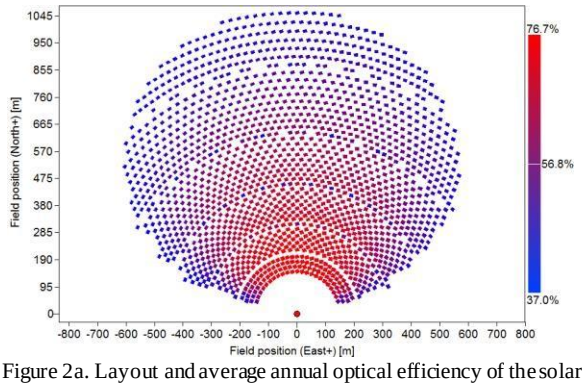

Figure 2a. Layout and average annual optical efficiency of the solar field installed at Bechar, Algeria.

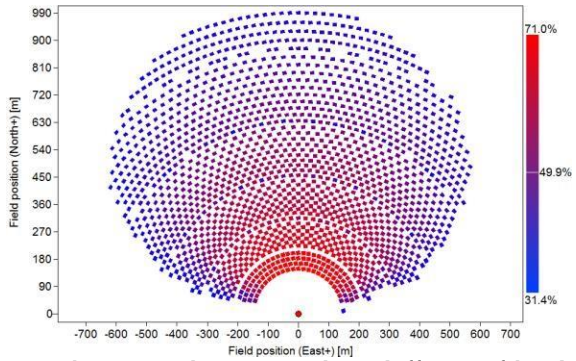

Figure 2b. Layout and average annual optical efficiency of the solar field installed at Oruro, Bolivia.

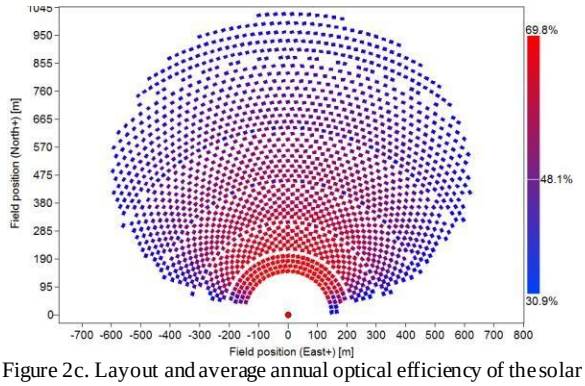

Figure 2c. Layout and average annual optical efficiency of the solar field installed at Antofagasta, Chile.

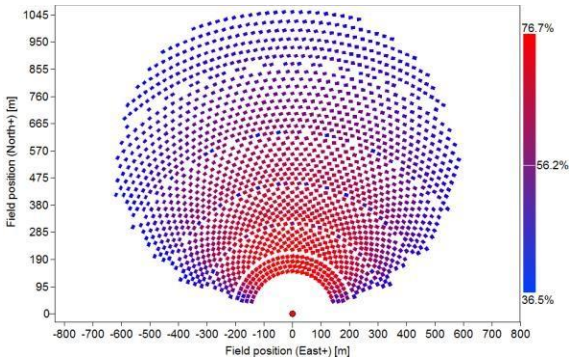

Figure 2d. Layout and average annual optical efficiency of the solar field installed at Sebha, Libya.

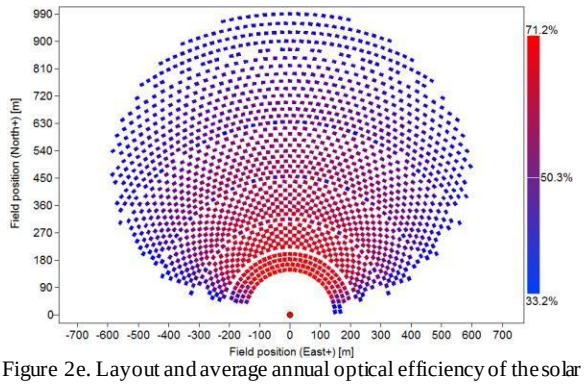

Figure 2e. Layout and average annual optical efficiency of the solar field installed at Arequipa, Peru.

Table 3 illustrates the nominal and annual optical efficiencies of the heliostat field at each site. There is a slight difference between the nominal efficiencies of the heliostat field at the selected locations. It varies from 59.5% at Sebha (Libya) to 62.1 at Arequipa (Peru). However, there is a significant difference between the annual optical efficiencies. The annual optical efficiency of a heliostat field installed in North Africa is so much higher than the annual optical efficiency of a heliostat field installed in South America. The highest annual optical efficiency of a solar field is observed at Bechar (Algeria) 56.8% followed by Sebha (Libya) 56.2 %. The lowest annual efficiency is observed at Antofagasta (Chile) 48.1%.

Table 3. The nominal and annual optical efficiency of the heliostat field at different locations.

Location	Country	Nominal optical efficiency (%)	Annual optical efficiency (%)
Bechar	Algeria	60.9	56.8
Oruro	Bolivia	61.5	49.9
Antofagasta	Chile	59.1	48.1
Sebha	Libya	59.5	56.2
Arequipa	Peru	62.1	50.3

Figure 3 shows the heat flux distribution at the receiver aperture, on March 21st at noon, for the five selected sites. The direct normal irradiance is 1 kW/m^2. The average heat flux at the receiver's aperture varies from 1147.6 to 1421.9 kW/m^2. This corresponds to an average heat flux on the receiver's absorptive surface of 376.26-463.28 kW/m^2.

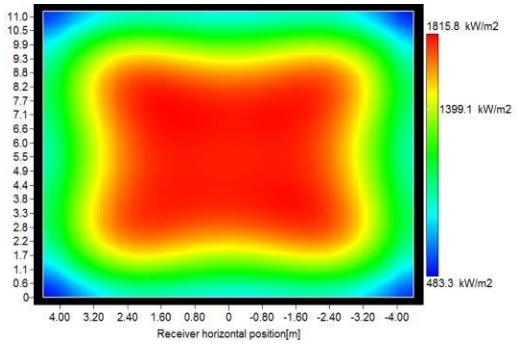

Figure 3a. Heat flux distribution at the aperture of the solar receiver for the case of Bechar (Algeria)

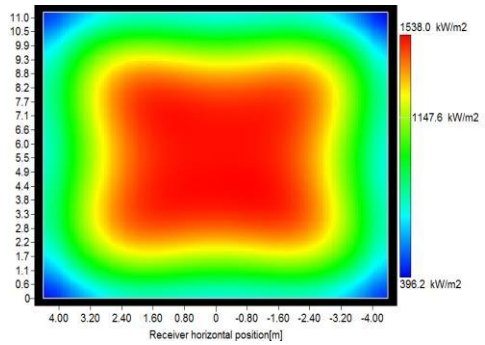

Figure 3b. Heat flux distribution at the aperture of the solar receiver for the case of Oruro (Bolivia)

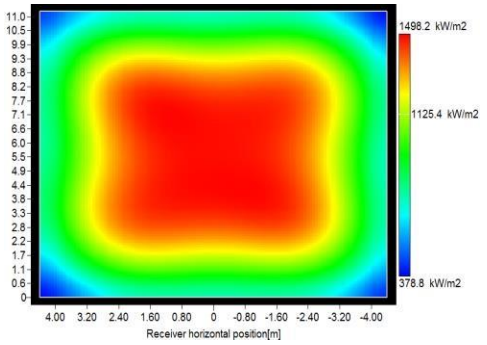

Figure 3c. Heat flux distribution at the aperture of the solar receiver for the case of Antofagasta (Chile)

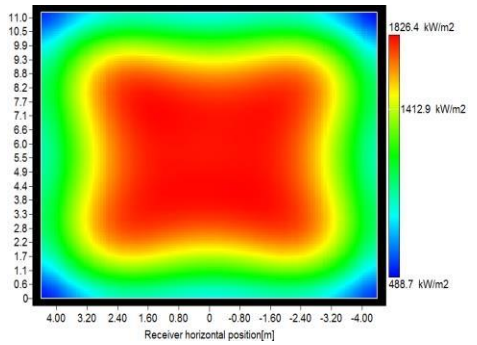

Figure 3d. Heat flux distribution at the aperture of the solar receiver for the case of Sebha (Lybia)

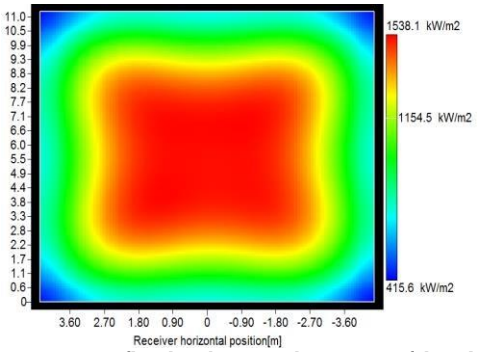

Figure 3e. Heat flux distribution at the aperture of the solar receiver for the case of Arequipa (Peru)

III.2. Results of the complete HSGT system

The Siemens SGT-800 gas turbine system of capacity 50 MWe is used as a case study in this work. The Brayton cycle design and operation parameters of this type of gas turbine is shown in Table 4.

Table 4. Gas turbine technical data.

Parameter	Value
Output power	ISO 50.5 MWe
Electrical efficiency	38.3%
Heat rate	9,407 kJ/kWh
Compressor pressure ratio	21.1:1
Exhaust gas flow	134.2 kg/s
Turbine inlet temperature	1237.6 °C
Exhaust temperature	553 °C

The HSGT system is simulated based on the results of the solar field and central receiver obtained in the previous section. These results are integrated with the design and operation parameters of SGT-800 gas turbine in the TRNSYS model. The gas turbine cycle efficiency of the all locations is presented in Figure 4. It can be noticed that the gas turbine efficiency at Atacama Desert (Cheli, Perue and Bolivia) is higher than Sahara region (Algeria and Libya) in which it is 40% and 39% respectively. This result is due to the fact that the annual

average ambient temperature at Atacama locations is lower than at Sahara Desert as can be seen in Table 5.

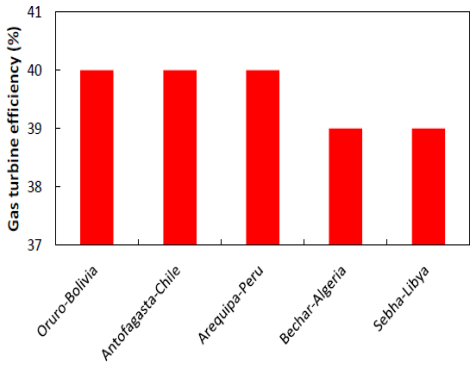

Figure 4. Gas turbine efficiency for the all locations

Table 5. Average annual ambient temperature.

Location	Average temperature
Oruro-Bolivia	5.8 °C
Antofagasta-Chile	16.8 °C
Arequipa-Peru	14.7 °C
Bechar-Algeria	22.4 °C
Sebha-Libya	23 °C

Figure 5 demonstrates the solar-to-electric efficiency of the HSGT system for the all locations. It can be noticed that the solar-to-electric efficiency at Atacama Desert is lower than in the Sahara Desert. In more details, in Atacama region the solar-to-electric efficiency varies from 17% at Antofagasta to about 18% in Arequipa. On the other hand, the efficiency of Sabha and Bechar is above 19.5%. The reason behind this is explained in the previous section in which the optical efficiency of the heliostat field in Sahara Desert is higher than in the Atacama region.

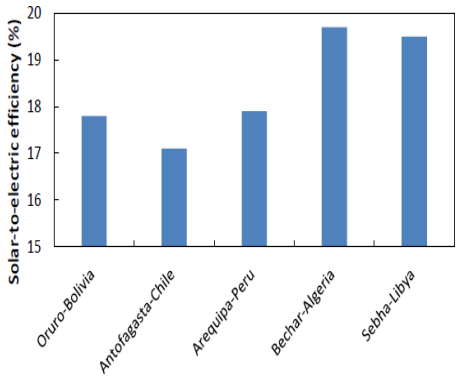

Figure 5. Solar-to-electric efficiency of HSGT

IV. Conclusion

This paper investigated the influence of the location on the performance of the hybrid solar gas turbine. An in-house code and two commercial software were used to provide a comprehensive study. Results showed that the location has a strong influence on the layout and the annual optical efficiency of the heliostat field.

The annual optical efficiency of a heliostat field in North Africa is higher than that in South America. The highest annual optical efficiency of a solar field is observed at Bechar (56.8%) while lowest is observed at Antofagasta (48.1%). However, because of the low ambient temperature at Atacama, the gas turbine efficiency at in Chlie, Perue and Bolivia is higher than Sahara (Algeria and Libya). Overall, the solar-to-electric efficiency at Atacama is lower than in the Sahara Desert. In Atacama the solar-to-electric efficiency varies from 17% to 18% while in Sahara it is above 19%.

Acknowledgements

This work was supported by La Agencia Nacional de Investigación y Desarrollo (ANID), project number ANID/FONDAP/ 15110019 “Solar Energy Research Center” SERC-Chile.

References

[1] B. Belgasim, Y. Aldali, M. J. R. Abdunnabi, G. Hashem, and K. Hossin, “The potential of concentrating solar power (CSP) for electricity generation in Libya,” *Renewable and Sustainable Energy Reviews*, Vol. 90. 2018, pp. 1–15.

[2] O. Behar, A. Khellaf, and K. Mohammedi, “A review of studies on central receiver solar thermal power plants,” *Renew. Sustain. energy Rev.*, Vol. 23, 2013, pp. 12–39.

[3] P. Heller *et al.*, “Test and evaluation of a solar powered gas turbine system,” *Sol. Energy*, Vol. 80, No. 10, 2006, pp. 1225–1230.

[4] P. Schwarzbözl *et al.*, “Solar gas turbine systems: Design, cost and perspectives,” *Sol. Energy*, Vol. 80, No. 10, 2006, pp. 1231–1240.

[5] “SOLGATE solar hybrid gas turbine electric power system. Technical Repor,” 2005.

[6] “Solar-Hybrid Power and Cogeneration Plants (SOLHYCO),” 2011.

[7] M. Quero, R. Korzynietz, M. Ebert, A. A. Jiménez, A. Del Río, and J. A. Brioso, “Solugas - Operation experience of the first solar hybrid gas turbine system at MW scale,” in *Energy Procedia*, Vol. 49, 2014, pp. 1820–1830.

[8] R. Korzynietz *et al.*, "Solugas - Comprehensive analysis of the solar hybrid Brayton plant," *Sol. Energy*, Vol. 135, 2016, pp. 578–589.

[9] B. Ssebabi, F. Dinter, J. van der Spuy, and M. Schatz, "Predicting the performance of a micro gas turbine under solar-hybrid operation," *Energy*, Vol. 177, 2019, pp. 121–135.

[10] S. Semprini, D. Sánchez, and A. De Pascale, "Performance analysis of a micro gas turbine and solar dish integrated system under different solar-only and hybrid operating conditions," *Sol. Energy*, Vol. 132, 2016, pp. 279–293.

[11] M. Babaelahi and H. Jafari, "Analytical design and optimization of a new hybrid solar-driven micro gas turbine/stirling engine, based on exergo-enviro-economic concept," *Sustain. Energy Technol. Assessments*, Vol. 42, 2020, pp. 100845.

[12] M. C. Cameretti, R. De Robbio, E. Pirone, and R. Tuccillo, "Thermo-Economic Analysis of a hybrid solar micro gas turbine power plant," in *Energy Procedia*, Vol. 126, 2017, pp. 667–674.

[13] M. Amelio, M. S. Pèrez, V. Ferraro, F. Rovense, and S. Bova, "Dynamic simulation of the temperature inlet turbine control system for an unfired micro gas turbine in a concentrating solar tower.," in *Energy Procedia*, Vol. 148, 2018, pp. 712–719.

[14] M. C. Cameretti, G. Langella, S. Sabino, and R. Tuccillo, "Modeling of a hybrid solar micro gas-turbine power plant," in *Energy Procedia*, Vol. 82, 2015, pp. 833–840.

[15] A. Giostri, M. Binotti, C. Sterpos, and G. Lozza, "Small scale solar tower coupled with micro gas turbine," *Renew. Energy*, Vol. 147, 2020, pp. 570–583.

[16] O. Behar, "A novel hybrid solar preheating gas turbine," *Energy Convers. Manag.*, Vol. 158, 2018, pp. 120–132.

[17] A. Giostri, "Preliminary analysis of solarized micro gas turbine application to CSP parabolic dish plants," in *Energy Procedia*, Vol. 142, 2017, pp. 768–773.

[18] A. M. Daabo, K. E. Hammo, O. A. Mohammed, A. A. Hassan, and T. Lattimore, "Performance investigation and design optimization of micro scale compressed air axial turbine for domestic solar powered Brayton cycle," *Sustain. Energy Technol. Assessments*, Vol. 37, 2020, pp. 100583, Feb.

[19] G. Barigozzi, G. Bonetti, G. Franchini, A. Perdichizzi, and S. Ravelli, "Thermal performance prediction of a solar hybrid gas turbine," *Sol. Energy*, Vol. 86, No. 7, 2012, pp. 2116–2127.

[20] B. Belgasim, O. Behar, M. Abdunnabi, and F. Mohamed, "Modeling and simulation of a large-scale hybrid solar gas turbine with pressurized air receiver," in *11th International Renewable Energy Congress, IREC 2020*, 2020.